PETROCHEMICAL CHARACTERISTICS AND GEOCHRONOLOGY OF THE IGNEOUS ROCKS IN BILIN AND ITS ENVIRONS, BILIN TOWNSHIP, MON STATE

Mya Moe Khaing[1], Hla Kyi[2], Thein Win[3]

Abstract

The research area is located in Bilin Township and its vicinity, Mon State. It lies between Lattitude 17˚12´45˝N to 17˚21´45˝N and Longitude 97˚09´00˝E to 97˚14´45˝E. The total area coverage is about 116.5 km^2. Four samples were sent to ALS laboratory of Geological Survey of Japan and analysed by XRF and LA-ICPMS. Eight samples were analyzed at DSSTRC (Defence Service Science and Technology Research Centre) in Pyin-Oo-Lwin Township and seven samples were sent to Geology Department, Mandalay University for XRF analysis. Geochemically, biotite granite, biotite-muscovite granite and biotite microgranite show chemical composition (weight percent) of SiO_2 (69.4 - 75.96), Al_2O_3 (13.34-16.8), TiO_2 (0.154-0.284), Na_2O+K_2O (7.765-10.31), Fe_2O_3+MgO (1.149-2.64), MnO (0.039-0.151), CaO (0.897-3.14) and P_2O_5 (0.027-0.159), suggesting calc-alkaline series and are predominantly peraluminous. Diorites and microdiorite exhibit SiO_2 (52.3-55.95), Al_2O_3 (17.69-22.3), TiO_2 (0.738-0.973), Na_2O+K_2O (4.95-6.364), Fe_2O_3+MgO (9.211-13.35), MnO (0.121-0.359), CaO (5.435-7.51) and P_2O_5 (0.285-0.602); proposing calc- alkaline series and are metaluminous. According to Harker's variation diagrams, TiO_2, Al_2O_3, Fe_2O_3, MnO, CaO, MgO and P_2O_5 are negatively correlated with SiO_2 and then Na_2O, K_2O are positively correlated with SiO_2. Result from geochemical analysis, biotite-muscovite granite and some biotite granites have high sodium content, normatic corundum ranges from 0.831 to 0.974 and biotite microgranite is low in sodium content, NaO_2 Vs K_2O diagram shows that the granitic rocks involve both I and S-types, Chappell and White (1994). Based on the tectonic discrimination diagram of Maniar and Piccoli (1989), the granitic rocks fall within the IAG+CAG+CCG field. In Y Vs Nb diagram; all the granitic rocks fall in the field of Syn-COLG and VAG. Y+Nb Vs Rb diagram indicates that all granites fall in the VAG field. U-Pb zircon dating of the biotite granite from the northern part of Lakhin pogoda gives the age of 51.9$\pm$0.7 Ma and suggests that the biotite granite was emplaced in Eocene.

Keywords; calc-alkaline, peraluminous, I-type, S-type, COLG, VAG, fractional crystallization

Introduction

The study area is chiefly covered by igneous and metasedimentary rocks, Fig (1). Igneous rocks are well exposed in the northern, north-western and south-eastern parts and metasedimentary rocks are cropped out in the central and western parts of the study area. Best exposure is observed along the stream sections and along the crest of the ridges.

[1] Dr, Associate Professor (Head), Department of Geology, Sittway University
[2] Part- Time Professor, Applied Geology Department, University of Yangon
[3] Professor, Pro-Rector (Retired), West Yangon University

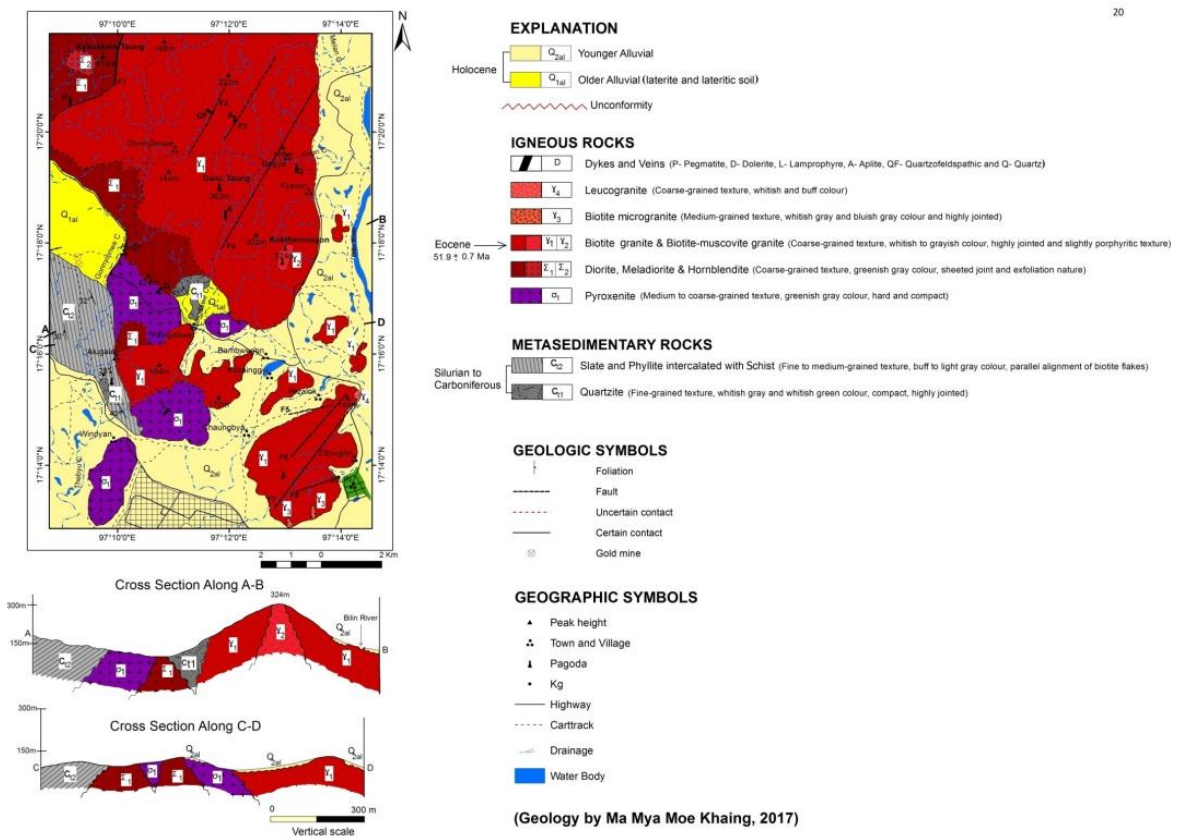

Figure 1 Geological Map of Bilin and its environment, Bilin Township, Mon State

Materials and Methods

The representative igneous rock samples including 6 biotite granites (sample no. KK-11, NG-23, mmk-1, mmk-5, mmk-11, mmk-13), 1 biotite-muscovite granite, (sample no. KK-04), 1 biotite microgranite, (sample no.15-26), 2 diorites, (sample no. R-01, KS-13), 1 microdiorite, (sample no. KS-04), 5 pyroxenites, (sample no. R-02, R-03, R-04, R-05, R-06), 1 hornblendite, (sample no. R-07), 2 lamprophyres (spessartite), (sample no.B-04, R-08) from the study area were selected for analysis. Four samples were sent to ALS laboratory of Geological Survey of Japan and analysed by XRF and LA-ICPMS. Eight igneous rock samples from the study area were analysed at DSSTRC (Defence Service Science and Technology Research Centre) in Pyin-Oo-Lwin Township and seven igneous rock samples were analysed at the Department of Geology, Mandalay University. The major oxide and trace elements abundance were determined by X-ray fluorescence spectrometry.

Results and Findings

The igneous rocks of the study area are biotite granites, biotite-muscovite granite, biotite microgranite, diorites, microdiorite, pyroxenites and hornblendite. The biotite granites, biotite-muscovite granite and biotite microgranite show chemical composition (weight percent) of SiO_2 (69.4 - 75.96), Al_2O_3 (13.34-16.8), TiO_2 (0.154-0.284), Na_2O+K_2O (7.765- 10.31), Fe_2O_3+MgO (1.149-2.64), MnO (0.039-0.151), CaO (0.897-3.14) and P_2O_5 (0.027-0.159) The chemical composition (weight percent) of diorites and microdiorite exhibit SiO_2 (52.3-55.95), Al_2O_3 (17.69-22.3), TiO_2 (0.738-0.973), Na_2O+K_2O (4.95-6.364), Fe_2O_3+MgO (9.211-13.35), MnO

(0.121-0.359), CaO (5.435-7.51) and P_2O_5 (0.285-0.602). Pyroxenites indicate SiO_2 (43.38-47.91), Al_2O_3 (13.10-25.56), TiO_2 (0.443-1.11), Na_2O+K_2O (2.005-4.74), Fe_2O_3+MgO (10.98-21.86), MnO (0.074-0.251), CaO (8.696-13.27) and P_2O_5 (0.060-0.421). Hornblendite illustrates the chemical composition (weight percent) of SiO_2 (43.81), Al_2O_3 (20.57), TiO_2 (1.07), Na_2O+K_2O (3.246), Fe_2O_3+MgO (16.96), MnO (0.127), CaO (11.89) and P_2O_5 (0.11). SiO_2 - Na_2O+K_2O - FeO_t+MgO diagram, (Fig. 2) shows the rise of SiO_2 and depletion of FeO_t + MgO during the entire process of magmatic differentiation. In Harker's variation diagram, Al_2O_3, TiO_2, Fe_2O_3, CaO, MgO, MnO and P_2O_5 are negatively correlated with SiO_2. Na_2O and K_2O are positively correlated with SiO_2. Plots of Harker's variation diagrams, selected trace elements of Ba, Sn, Nb, Zn, Rb, Zr, Y and Mo are positively correlated with SiO_2. Plots of trace elements Sr, Ni, Ce versus SiO_2 show decreasing of those elements with increasing of SiO_2 contents, Fig (3). The normative anorthite content against the Thornton and Tuttle Differentiation Index (TTDI) diagram show the degree of differentiation, the hornblendite and diorite contain proportionately more normative anorthite in plagioclase than the biotite granite, shown in Fig (4). Na_2O+K_2O/Al_2O_3 Vs SiO_2 variation diagram, Fig (5) and K_2O Vs SiO_2, Fig (6) show the trend of magmatic differentiation. Plot of alkali (Na_2O + K_2O) versus silica (SiO_2) diagram, Fig (7) exhibits the granitic rocks in the study area fall in the subalkaline series. K_2O Vs Na_2O diagram, Fig (8) shows that the granitic rocks of the study area involve both I-type and S-type. TAS diagram after Cox et. al. (1979), Fig (9) indicates four groups of igneous and the dividing line between alkaline and subalkaline magma series. The igneous rocks from the study area generally range from acid to ultrabasic group and belong to the subalkaline affinity. The granites are predominantly peraluminous with high Aluminum Saturation Indexes (ASI) of A/NK (Molecular Al_2O_3/Na_2O+K_2O) and A/CNK (Molecular Al_2O_3/ CaO +Na_2O+K_2O) ranging from 1.384 to 1.879 and from 1.054 to 1.524, respectively. In the Na_2O - Al_2O_3 - K_2O diagram, the granitic rocks in the study area fall in the peraluminous field. Diorite and microdiorite fall in the metaluminous field.

Genetic Type of Granitoid Rocks

Geochemical analysis data, Table (1) have been plotted on a various diagram to distinguish I and S type granitic rocks. K_2O Vs Na_2O diagram show that the granitic rocks of the study area involve both I-type and S-type. Some biotite granites are relatively high in sodium, Na_2O normally $> 3.2\%$ in the range of (3.57%-3.93%) with approximately 5% K_2O and one biotite granite and one biotite-muscovite granite from Koktheinnayon pagoda are low in sodium, Na_2O normally $< 3.2\%$, their content are 2.72% and 3.072%. The normative corundum ranges from 0.757 - 0.974. Only biotite microgranite is sodium low, Na_2O (2.86%), it is generally < 3.2%. Lack of normative magnetite is characteristic of S-type. Above these facts, the granitic rocks in the study area are I and S-types granite according to Chappell and White (1974). The relatively high quartz content, up to 35.24 wt% of this S type granite can be considered that this granite was derived from the quartz rich sedimentary rocks. It may be formed from the supracrustal origin (Chappell and White, 2001).

Table 1 Major oxide and trace elements abundances of the igneous rocks from the study area

Sample No	KK-11	15-26	NG-23	KK-04	mmk-1	mmk-5	mmk -11	mmk-13	R-04	R-08
SiO_2	71.9	69.7	69.4	70.5	75.96	72.5	75.73	74.2	48.8	51.93
TiO_2	0.159	0.284	0.213	0.202	0.154	0.266	0.161	0.204	0.67	0.637
Al_2O_3	15.2	13.9	16.8	16	13.65	14.59	13.34	14.43	19.4	14.5
Fe_2O_3	1.13	2.39	0.855	1.19	0.973	2.076	1.057	1.525	10.5	9.694
MnO	0.059	0.078	0.068	0.151	0.039	0.065	0.06	0.048	0.237	0.155
MgO	0.326	0.256	0.294	0.323	0.273	0.56	0.309	0.456	4.39	7.059
CaO	1.58	3.14	1.59	1.29	1.01	1.809	0.897	1.618	7.69	7.568
Na_2O	2.72	2.86	3.78	3.072	3.577	3.933	3.695	3.743	4.29	3.03
K_2O	6.79	7.18	6.53	6.27	4.55	3.832	4.58	4.225	3.56	2.91
P_2O_5	0.106	0.159	0.141	0.139	0.027	0.064	0.031	0.052	0.266	0.522
Total	99.93	99.94	99.67	99.88	100	99.7	99.87	100.5	99.7	97.98
A/CNK	1.375	1.056	1.411	1.405	1.472	1.524	1.455	1.504	1.264	1.075
A/NK	1.598	1.384	1.639	1.585	1.655	1.879	1.612	1.809	2.471	2.661
Sn	15.51	8.884	15.97	-	6.969	15.48	-	11.54	-	-
Cd	47.89	29.22	50.34	23.18	20.05	30.37	8.348	25.17	2.814	1.586
Ag	22.3	11.63	24.88	13.4	-	23.68	-	18.34	3.871	3.294
Pd	46.89	38.21	59.18	20.87	29.84	34.9	14.36	28.99	3.894	2.687
Rh	40.64	20	36.66	27.66	14.12	28.58	5.199	22.7	1.267	-
Ru	6.646	4.36	6.907	4.164	2.381	5.912	-	4.349	-	-
Mo	6.035	4.79	5.884	3.748	5.154	5.006	3.767	4.894	0.062	0.067
Nb	8.526	8.066	13.21	8.34	5.92	4.762	3.691	4.317	0.051	0.069
Pb	19.19	19.71	30.11	26.49	44.15	8.618	8.714	9.245	6.635	2.352
Ga	8.812	8.855	7.864	6.026	-	4.621	3.46	3.037	-	0.01
Zn	6.667	6.103	6.398	10.1	17.45	9.104	15.94	6.858	6.278	11.08
Cu	-	-	6.051	3.929	6.324	4.052	5.859	3.308	5.743	3.882
Co	-	4.79	-	11.68	5.474	0	7.087	5.25	10.39	9.587
Fe	714.4	789.9	650.9	764.5	774.5	771.4	868	797.2	919	897
Mn	36.41	30.82	61.8	55.47	34.67	30.91	33.1	35.64	17.55	21.7
Ti	-	-	-	-	-	-	-	-	14.14	19.83
Nd	0.334	0.492	0.314	0.315	0.388	0.245	0.652	0.395	0.725	0.84
Pr	0.223	0.369	0.236	0.2	-	0.185	0.299	0.196	0.51	0.534
Ce	16.68	26.42	17.1	14.35	16.55	12.65	24.19	17.1	29.8	37.3
La	0.174	0.247	0.138	0.106	-	0.152	0.206	0.217	0.295	0.211
Ba	314.8	338.3	178.3	169.9	543.6	767.6	611.7	686.3	0.398	0.311
Sb	-	0.022	0.028	0.088	2.013	0.164	0.594	0.422	0.075	0.212
Zr	64.22	38.24	23.57	69.11	59.92	99.15	108.2	105.21	36.96	63.69
Y	1.84	-	2.08	5.87	2.04	2.66	1.86	-	1.72	2.15
Sr	62.38	72.06	26.21	69.22	88.88	176.9	163.2	177.1	306.7	675.4
Rb	86.18	90.21	128.9	90.87	57.4	48.08	48.27	66.02	28.18	27.33
Cs	4.646	6.628	2.801	7.136	13.95	9.559	10.86	9.765	38.12	58.51
K	20.48	22.15	21.64	20.27	23.28	20.66	20.33	17.32	11.46	11.47
Al	1.3	1.839	1.801	1.338	2.022	1.854	1.927	1.55	19.22	23.14
Si	24.06	25.31	31.36	23.7	24.26	26.15	20.72	28.54	19.91	19.11
Cl	1.67	1.434	1.805	1.686	0.889	1.148	1.131	0.957	29.15	25.29
S	0.718	0.594	0.713	0.609	13.85	2.959	7.203	7.372	7.08	15.3

Sample No	KS-04	R-01	KS-13	R-02	R-03	R-04	R-05	R-06	R-07
SiO_2	52.3	55.95	53.1	45.84	46.28	43.48	47.38	47.91	43.81
TiO_2	0.973	0.75	0.738	0.56	0.506	1.11	0.735	0.663	1.07
Al_2O_3	22.3	17.69	18	13.1	23.26	18.08	25.56	16.5	20.57
Fe_2O_3	8.25	6.24	9.4	13.06	6.097	13.61	7.65	8.886	10.67
MnO	0.359	0.121	0.21	0.251	0.086	0.164	0.074	0.196	0.127
MgO	2.92	2.971	3.95	8.8	6.262	7.411	3.52	7.741	6.297
CaO	7.39	5.435	7.51	9.694	11.34	11.33	13.27	8.696	11.89
Na_2O	2.69	4.034	1.98	3.26	3.01	1.6	1.79	2.63	2.65
K_2O	2.26	2.33	4.27	1.68	0.331	0.605	0.291	1.15	0.596
P_2O_5	0.347	0.285	0.602	0.621	0.087	0.062	0.06	0.233	0.11
Total	99.79	95.81	99.76	96.47	97.26	97.33	96.16	94.37	97.79
A/CNK	1.807	1.499	1.308	0.907	1.584	1.355	1.665	1.322	1.359
A/NK	4.505	2.779	2.88	2.763	6.961	9.017	12.28	4.365	6.337
Sn	-	-	0.896	-	1.573	-	-	0.866	0.695
Cd	3.002	4.639	3.378	2.766	6.316	2.199	1.51	3.458	2.073
Ag	3.847	5.742	5.692	4.549	5.976	3.625	3.669	4.556	3.691
Pd	4.698	5.987	4.574	4.299	7.321	3.328	2.786	4.177	3.354
Rh	0.908	3.992	1.973	1.34	4.708	0.621	-	1.653	0.506
Ru	0.36	0.7	0.651	0.29	0.966	0.307	-	0.399	-
Mo	0.784	0.881	0.628	0.524	2.092	0.669	0.298	0.779	0.464
Nb	0.719	0.573	0.571	0.65	1.878	0.599	0.329	0.743	0.461
Pb	4.032	5.975	1.898	3.433	3.654	1.426	0.805	1.647	0.827
Ga	1.575	1.985	1.513	1.295	2.341	0.685	-	0.909	1.286
Zn	10.39	4.856	4.454	5.657	6.573	6.765	5.218	3.682	5.631
Cu	3.471	2.639	12.7	5.817	8.012	3.069	4.884	1.97	1.841
Ni	-	-	-	3.712	4.089	3.521	3.088	3.487	3.038
Co	10.95	8.302	5.854	9.459	7.996	7.57	6.889	7.97	6.599
Fe	899.6	922	913.7	917.7	899.8	929.1	937.4	920.4	917.9
Mn	27.63	12.87	9.272	20.34	17.12	15.33	14.81	13.46	11.13
Ti	27.34	13.31	26.86	14.5	17.69	19.34	15.35	17.69	28.82
Nd	0.76	0.756	0.774	0.707	0.656	0.926	0.992	0.829	0.957
Pr	0.507	0.42	0.48	0.437	0.461	0.603	0.616	0.393	0.599
Ce	31.62	32.92	22.66	23.66	22.33	35.61	39.92	26.91	33.01
La	0.308	0.312	0.263	0.276	0.233	0.346	0.333	0.262	0.362
Ba	494	257.6	218.7	228.3	374.6	462.8	375.7	643.6	388.8
Sb	0.038	0.122	-	0.051	0.055	0.060	-	-	-
Zr	69.63	16.12	28.8	25.72	103.9	57.56	-	55.99	36.21
Y	2.18	-	-	-	2.3	2.17	2.22	1.91	2.67
Sr	332.9	448.2	565.9	405.58	534.6	567.2	563.2	629.4	512.5
Rb	33.63	6.64	3.5	9.84	25.63	23.81	7.67	31.35	0
Cs	37.34	66.01	75.82	69.19	28.4	38.26	75.82	38.78	61.19
K	8.605	1.962	2.505	6.255	15.18	16.46	2.616	20.05	3.597
Al	3.522	3.827	4.55	3.201	1.606	2.338	3.14	3.16	4.052
Si	25.31	27.11	26.08	24.77	18.85	15.95	21.24	29.02	23.72
Cl	1.643	2.812	2.063	3.036	1.391	1.647	1.762	2.38	2.942
S	0.609	0.838	0.989	0.996	1.337	0.435	0.743	0.613	1.162

Condition during Crystallization of the Granitic Rocks

Normative data plot of Quartz - Albite - Orthoclase diagram after Tuttle and Bowen (1985), H_2O saturated liquidus field boundaries in the system for various water pressures. This diagram, Fig (10) indicates the granitic rocks in the study area lie within 2kb and 10 kb during crystallization. It can be suggested that the granitic rocks from the study area were consolidated under the low pressure condition. If the igneous rocks were assumed as crystallization at minimum pressure of 2kb, their liquid temperature can be estimated from the diagram showing the relationship between differentiation index and temperature at 2 kb water pressure.

Depth of the crystallization of the igneous rocks can be expressed from the schematic depth-temperature diagram (after Marmo, 1969), Fig (11). From this diagram, the liquidus temperatures are 680˚C to 712˚C, 690˚C, 700˚C for biotite granites, biotite-muscovite granite, biotite microgranite. Diorites and microdiorite crystallized at 750˚C to 760˚C, 760˚C and then pyroxenites at 870˚C to 940˚C. Generally, it may be suggested that biotite granites, biotite-muscovite granite and biotite microgranite may crystallized at the depth of 22km to 24km, 24km, 22km. Diorites and microdiorite may differentiated at 25km and pyroxenites may be at the depth between 30 km to 33 km.

Tectonic Discrimination of the Granitoid Rocks

The configurations of tectonic environments for the granitic rocks of the study area were made by using Maniar and Piccoli (1989) classification schemes. SiO_2 versus K_2O diagram are shown to classify the tectonic environment into IAG+CAG+CCG+CEUG+POG +RRG and OP field. The granitic rocks of the study area fall within the IAG+CAG+CCG +CEUG+POG field. In plots of M/AFM (MgO/Al_2O_3 +FeO +MgO) versus F/AFM (FeO /Al_2O_3 +FeO +MgO) variation diagram and plots of C/ACF (CaO /Al_2O_3 +CaO + FeO) versus F/ACF (FeO/ Al_2O_3+CaO+FeO) variation diagram show the granitoid rocks of the study area fall within the IAG+CAG+CCG field. Again in the Shand's Index diagram, plots of the granitic rocks fall in the CAG and CCG field, Fig (12, A). According the above mentioned data, it can be safely considered that the granitoid rocks of the study area are orogenic granitoids. Therefore, the granitic rocks of the biotite granites, biotite-muscovite granite and biotite microgranite were formed on the continent relation to the subduction of an oceanic plate beneath the continent. Pearce et al (1984) postulated that the discrimination diagram to integrate granite geochemistry into the plate tectonic framework. In the Y versus Nb diagram; all granites in the study area fall in the field of Syn-COLG and VAG and Y+Nb versus Rb diagram indicates that all granite rocks are fitted in the VAG field. According to the above data, the syn-collision granites support mantle of crustal sources augmented by melt and fluids from subducted continental crust. The volcanic arc granite is generally depleted mantle sources enriched by a subduction fluid $\pm$ interaction with continental crust. Batchelor and Bowden (1985) used to discriminate the tectonic setting of granite according to R_1-R_2 binary (millication) diagram; Fig (12, B) indicates the granitoid rocks of the study area correspond to syn-collision zone.

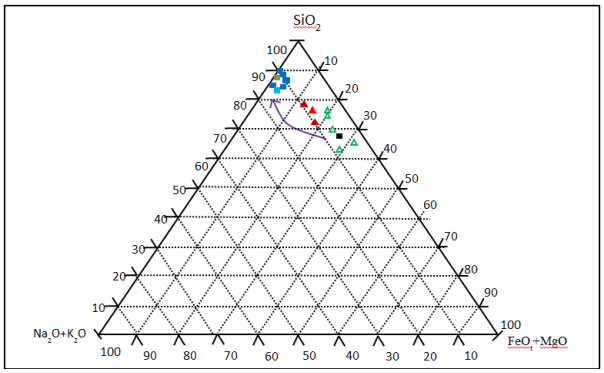

Figure 2 SiO_2 - (Na_2O+K_2O)-(FeO+MgO) diagram showing the evolutionary trend of the gneous rocks (after Le Meitre, 1989)

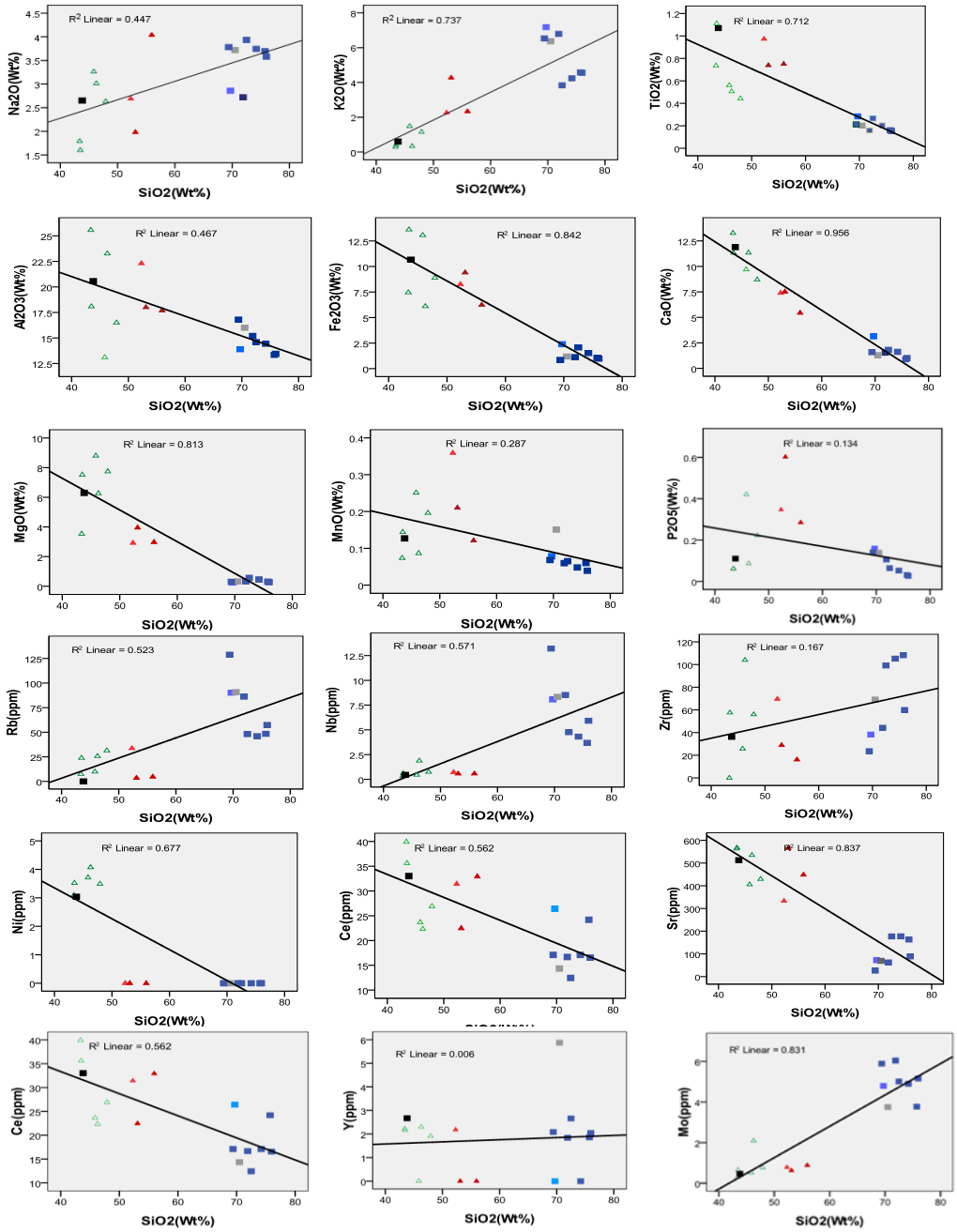

Figure 3 Harker's variation diagrams showing the correlation between major oxides and trace elements Vs SiO_2 of the igneous rocks from the study area, Symbols as in Table (1)

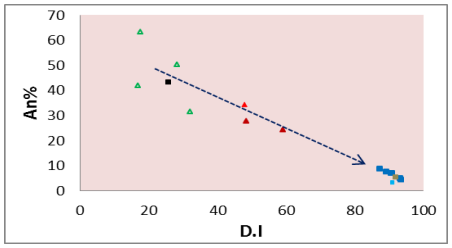

Figure 4 Anorthite percent (An%) in normative plagioclase plotted against Differentiation Index (D.I) of Thornton and Tuttle (1960). Symbols as in Table (1)

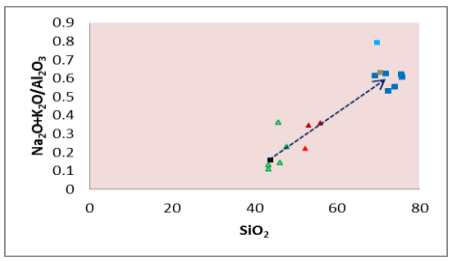

Figure 5 Na_2O+K_2O/Al_2O_3 Vs SiO_2 variation diagram, showing the trend of differentiation (after Chappell and White, 1974), Symbols as in Table (1)

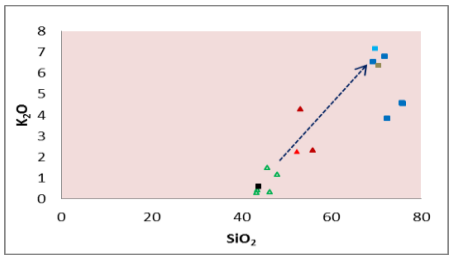

Figure 6 K_2O Vs SiO_2 variation diagram, showing the trend of differentiation (after Le Maitre, 2001), Symbols as in Table (1)

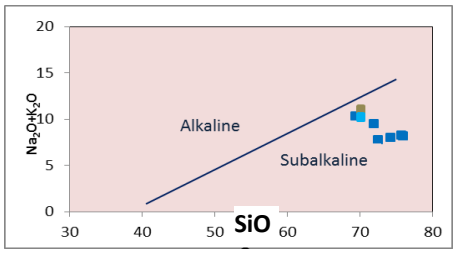

Figure 7 Na_2O+K_2O Vs SiO_2 diagram distinguishing between alkaline and subalkaline series, (after MacDonald, 1968). The granitic rocks in the study area fall in the subalkaline series of the study area, Symbols as in Table (1).

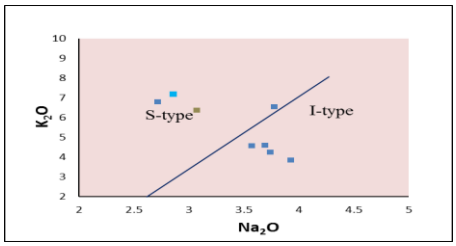

Figure 8 K_2O Vs Na_2O diagram for the granitic rocks of the study area, (after Chappell and White, 1983)

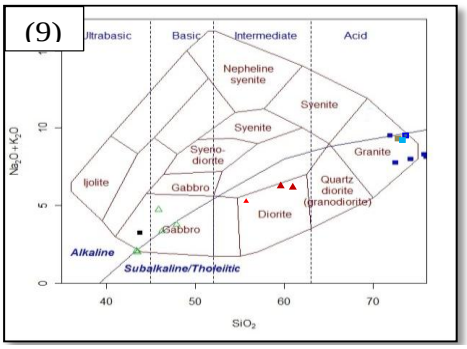

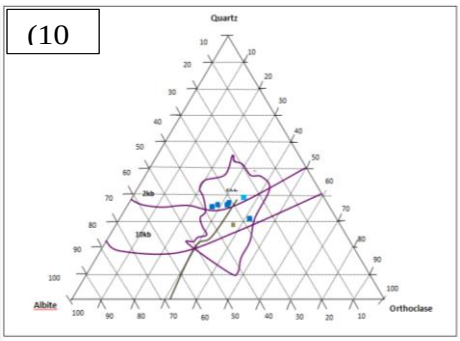

Figure 9 TAS diagram of Cox et. al. (1979) showing subalkaline series of the study area, Symbols as in Table (1)

Figure 10 Normative data plot of Quartz - Albite - Orthoclase ratio exhibits the granitic rocks in the study area have water pressure within 2 kb and 10 kb (after Tuttle and Bowen, 1985), Symbols as in Table (1)

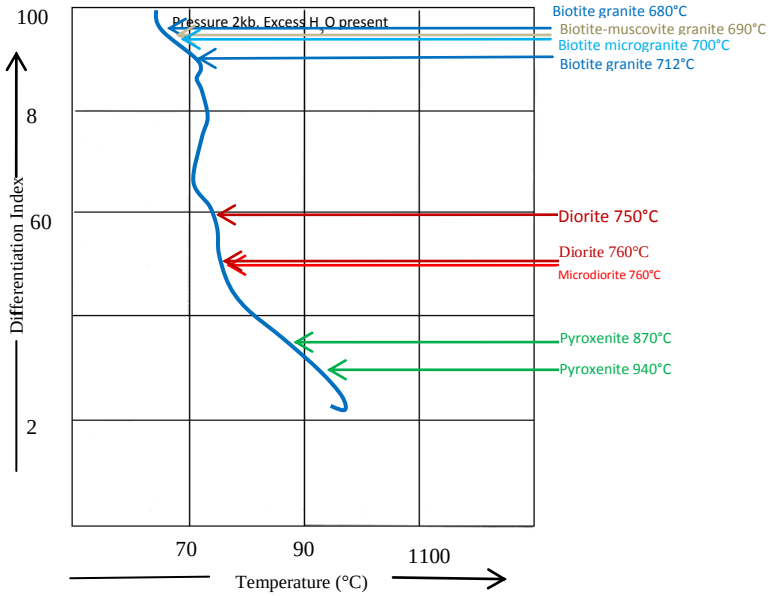

Figurer 11 Temperature-differentiation index diagram for the igneous rocks of the study area, at 2 kb water pressure (after Piwinskii and Wyllie, 1970)

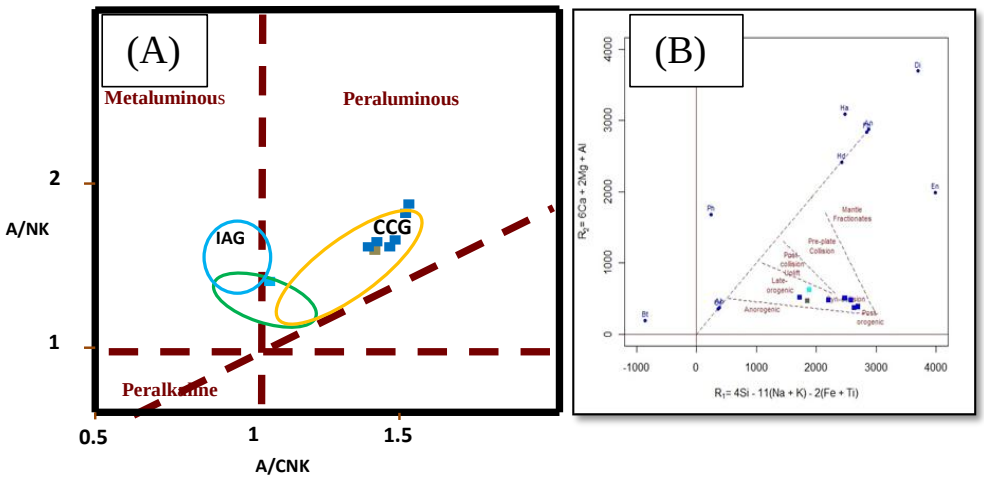

Figure 12 (A)Shand's Index diagram for granitic rocks of study area, which fall within the CAG and CCG field, Symbols as in Table (1) (B) R_1-R_2 binary (millication) diagram indicates the granitoid rocks of the study area correspond to syn-collision zone

Geochronology of the igneous rock of the study area

Biotite granite (MMK-5) cropped out at the northern part of Lakhin pogoda, Lattitude N 17˚14′16″, Longitude E 97˚12′ 46″ was sent to the geochemical and isotope laboratory at the ALS laboratory of Geological Survey of Japan for LA-ICPMS. Biotite granite gives the zircons age of 51.9±0.7 Ma, Fig (13). The result from zircon crystallization suggests that the biotite granite was emplaced in Eocene.

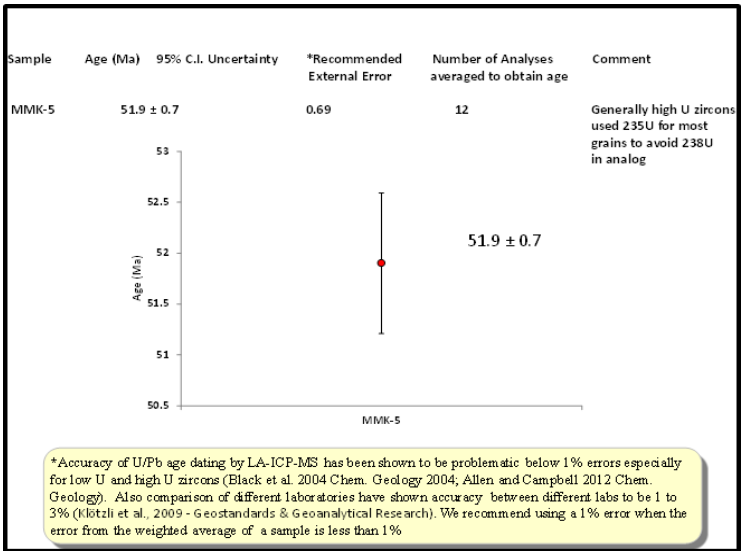

Figure 13 Result of biotite granite at Latitude N 17˚ 14′ 16″, Longitude E 97˚ 12′ 46″, Accuracy of U/Pb age dating by using LA-ICPMS technique

Conclusion

Geologically, the study area is chiefly covered by igneous and metasedimentary rocks. Geochemically, plots of Harker's variation diagrams selected on major oxides and trace elements, Al_2O_3, TiO_2, Fe_2O_3, CaO, MgO, MnO and P_2O_5 are negatively correlated with SiO_2. Na_2O and K_2O are positively correlated with SiO_2. Ba, Sn, Nb, Zn, Rb, Zr, Y and Mo are positively correlated with SiO_2. Sr, Ni, Ce versus SiO_2 show decreasing of those elements with increasing of SiO_2 contents. The normative anorthite content against the Thornton and Tuttle Differentiation Index (TTDI) diagram, hornblendite and diorite contain proportionately more normative anorthite in plagioclase than the biotite granite. If the igneous rocks were assumed as crystallization at 2 kb water pressure, the liquidus temperatures are 680˚C to 712˚C, 690˚C, 700˚C for biotite granites, biotite-muscovite granite, biotite microgranite. Diorites and microdiorite crystallized at 750˚C to 760˚C, 760˚C and then pyroxenites at 870˚C to 940˚C.Depth of the crystallization of the igneous rocks can be expressed from the schematic depth-temperature diagram (after Marmo, 1969), biotite granites, biotite-muscovite granite and biotite microgranite may crystallized at the depth of 22km to 24km, 24km and 22km. Diorites and microdiorite may differentiated at 25km and pyroxenites may be at the depth of 30 km to 33 km. According to Maniar and Piccoli (1989) diagrams; the granitic rocks of the study area fall in the IAG + CAG + CCG field. It can be safely considered that the granitoid rocks of the study area are Orogenic granitoids. Therefore, the granitic rocks of the biotite granites, biotite-muscovite granite and biotite microgranite were formed on the continent relation to the subduction of an oceanic plate beneath the continent. The tectonic setting of granite according to R_1-R_2 binary (millication) diagram indicates the granitoid rocks of the study area correspond to syn-collision zone. Radiometric dating by zircon U-Pb method indicates that the age of biotite granite gives the zircons age of 51.9$\pm$0.7 Ma. The result from zircon crystallization suggests that the biotite granite was emplaced in Eocene. According to Chappell and White (1974), the genetic types of granitic rocks of the study area are regarded as both I-type and S-type. S-type granites probably originated from the remelting of metasediments and I- type granites derived from the remelting of deep-seated igneous materials. Biotite granite contain two mica are considered as sedimentary protolith of S-type and some biotite granite are I-type. Harker's variation diagrams are not only

linear but also irregular or scatter. Binary plots of Na_2O Vs K_2O diagram of Chappell and White (1983) shows that the granitic rocks of the study area involve both I-type and S-type.

Acknowledgements

My deepest thanks to U Aung Kyaw Htoon, Part-Time Lecturer, Geology Department, Dagon University for providing collected data for my research.

References

Chappell.B.W, White. A.J.R, (2001). Two contracting granite types : 25 years later, *Australian Journal of Earth Science* (2001) 48. 489-499

Chhibber.H.L., (1934). *The Geology of Burma*, Macmillan & Co.Ltd., London.

Fryer, B.J., Jackson, S.E., Longerich, H.,P.(1993). *The application of Laser Ablation Microprobe-Inductively Coupled Plasma-Mass Spectrometry (LAM-ICP-MS) to insitu U-Pb Geochronology*, Chemical Geology, 109, p.1-8.

Khin Zaw, (1990). Geological, Petrological, and Geochemical characteristics of granitoid rocks in Burma, with special reference to the associated of W-Sn mineralization and their tectonic *setting, Journal of Southeast Asian Earth Sciences. Vol.4.*

Le Maitre, R. W. (2001). *Igneous rocks; A classification and Glossary of Term*. 2nd ed., Recommendation of the International Union of Geological Science Subcommission on the systematic of igneous rocks. Cambridge University Press.

Maniar, P.D, Piccoli., P.M. (1989). *Tectonic discrimination of Granitoids*. G.A.S. Bull., volume.101, p.635-643

Marmo,V., (1956). *On the emplacement of Granites*. Am. Journal of Science. volume-254. p.479- 492

Middlemost, E.A.,(1994). *Naming material in the magma/igneous rock system. Earth Science reviews*, 37(3), p.215-244

Pearce. J. A., Harris, N.W.,Tindle, A.G.,(1984). Trace element discrimination diagrams for the tectonic interpretation of granitic rocks. *Journal of Petrology* 25.p. 956-983.

Rollinson,H.R,(1993), *Using Geochemical data: evaluation, presentation, interpretation*, Longman Group UK Ltd. P.48-80

Rollinson, H.R, (1994), *Using Geochemical data: evaluation, presentation, interpretation*, Longman Group UK Ltd. P.352.

Thornton,C,P.,and Tuttle, O.F.,(1960).Chemistry of Igneous Rocks. Diffierentiation index. *Am.Journal of Science*, volume 258, p.664-684.